

## PUBLISHED VERSION

H.E.S.S. Collaboration, A. Abramowski...P. Dewilt...N. Maxted...G. Rowell...et al.  
**H.E.S.S. observations of the Crab during its March 2013 GeV gamma-ray flare**  
Astronomy and Astrophysics, 2014; 562(02):1-5

© ESO 2014. Article published by EDP Sciences

Originally published: <https://doi.org/10.1051/0004-6361/201323013>

### PERMISSIONS

[https://www.aanda.org/index.php?option=com\\_content&view=article&id=863&Itemid=295](https://www.aanda.org/index.php?option=com_content&view=article&id=863&Itemid=295)

### Green Open Access

The Publisher and A&A encourage arXiv archiving or self-archiving of the final PDF file of the article exactly as published in the journal and without any period of embargo.

**20 September 2018**

<http://hdl.handle.net/2440/82896>

LETTER TO THE EDITOR

## H.E.S.S. observations of the Crab during its March 2013 GeV gamma-ray flare

H.E.S.S. Collaboration, A. Abramowski<sup>1</sup>, F. Aharonian<sup>2,3,4</sup>, F. Ait Benkhali<sup>2</sup>, A. G. Akhperjanian<sup>5,4</sup>, E. Angüner<sup>6</sup>, G. Anton<sup>7</sup>, S. Balenderan<sup>8</sup>, A. Balzer<sup>9,10,\*</sup>, A. Barnacka<sup>11</sup>, Y. Becherini<sup>12</sup>, J. Becker Tjus<sup>13</sup>, K. Bernlöhr<sup>2,6</sup>, E. Birsin<sup>6</sup>, E. Bissaldi<sup>14</sup>, J. Biteau<sup>15</sup>, M. Böttcher<sup>16</sup>, C. Boisson<sup>17</sup>, J. Bolmont<sup>18</sup>, P. Bordas<sup>19</sup>, J. Brucker<sup>7</sup>, F. Brun<sup>2</sup>, P. Brun<sup>20</sup>, T. Bulik<sup>21</sup>, S. Carrigan<sup>2</sup>, S. Casanova<sup>16,2</sup>, M. Cerruti<sup>17,22</sup>, P. M. Chadwick<sup>8</sup>, R. Chalme-Calvet<sup>18</sup>, R. C. G. Chaves<sup>20</sup>, A. Cheesebrough<sup>8</sup>, M. Chrétien<sup>18</sup>, S. Colafrancesco<sup>23</sup>, G. Cologna<sup>24</sup>, J. Conrad<sup>25,26</sup>, C. Couturier<sup>18</sup>, Y. Cui<sup>19</sup>, M. Dalton<sup>27,28</sup>, M. K. Daniel<sup>8</sup>, I. D. Davids<sup>16,29</sup>, B. Degrange<sup>15</sup>, C. Deil<sup>2</sup>, P. deWilt<sup>30</sup>, H. J. Dickinson<sup>25</sup>, A. Djannati-Atai<sup>31</sup>, W. Domainko<sup>2</sup>, L. O'C. Drury<sup>3</sup>, G. Dubus<sup>32</sup>, K. Dutson<sup>33</sup>, J. Dyks<sup>11</sup>, M. Dyrda<sup>34</sup>, T. Edwards<sup>2</sup>, K. Egberts<sup>14</sup>, P. Eger<sup>2</sup>, P. Espigat<sup>31</sup>, C. Farnier<sup>25</sup>, S. Fegan<sup>15</sup>, F. Feinstein<sup>35</sup>, M. V. Fernandes<sup>1</sup>, D. Fernandez<sup>35</sup>, A. Fiasson<sup>36</sup>, G. Fontaine<sup>15</sup>, A. Förster<sup>2</sup>, M. Füßling<sup>10</sup>, M. Gajdus<sup>6</sup>, Y. A. Gallant<sup>35</sup>, T. Garrigoux<sup>18</sup>, G. Giavitto<sup>9</sup>, B. Giebels<sup>15</sup>, J. F. Glicenstein<sup>20</sup>, M.-H. Grondin<sup>2,24</sup>, M. Grudzińska<sup>21</sup>, S. Häffner<sup>7</sup>, J. Hahn<sup>2</sup>, J. Harris<sup>8</sup>, G. Heinzlmann<sup>1</sup>, G. Henri<sup>32</sup>, G. Hermann<sup>2</sup>, O. Hervet<sup>17</sup>, A. Hillert<sup>2</sup>, J. A. Hinton<sup>33</sup>, W. Hofmann<sup>2</sup>, P. Hofverberg<sup>2</sup>, M. Holler<sup>10</sup>, D. Horns<sup>1,\*</sup>, A. Jacholkowska<sup>18</sup>, C. Jahn<sup>7</sup>, M. Jamroz<sup>37</sup>, M. Janiak<sup>11</sup>, F. Jankowsky<sup>24</sup>, I. Jung<sup>7</sup>, M. A. Kastendieck<sup>1</sup>, K. Katarzyński<sup>38</sup>, U. Katz<sup>7</sup>, S. Kaufmann<sup>24</sup>, B. Khélifi<sup>31</sup>, M. Kieffer<sup>18</sup>, S. Klepser<sup>9</sup>, D. Klochkov<sup>19</sup>, W. Kluzniak<sup>11</sup>, T. Kneiske<sup>1</sup>, D. Kolitzus<sup>14</sup>, Nu. Komin<sup>36</sup>, K. Kosack<sup>20</sup>, S. Krakau<sup>13</sup>, F. Krayzel<sup>36</sup>, P. P. Krüger<sup>16,2</sup>, H. Laffon<sup>27</sup>, G. Lamanna<sup>36</sup>, J. Lefaucheur<sup>31</sup>, A. Lemièrre<sup>31</sup>, M. Lemoine-Goumard<sup>27</sup>, J.-P. Lenain<sup>18</sup>, D. Lennarz<sup>2</sup>, T. Lohse<sup>6</sup>, A. Lopatin<sup>7</sup>, C.-C. Lu<sup>2</sup>, V. Marandon<sup>2</sup>, A. Marcowith<sup>35</sup>, R. Marx<sup>2</sup>, G. Maurin<sup>36</sup>, N. Maxted<sup>30</sup>, M. Mayer<sup>10</sup>, T. J. L. McComb<sup>8</sup>, J. Méhault<sup>27,28</sup>, P. J. Meintjes<sup>39</sup>, U. Menzler<sup>13</sup>, M. Meyer<sup>25</sup>, R. Moderski<sup>11</sup>, M. Mohamed<sup>24</sup>, E. Moulin<sup>20</sup>, T. Murach<sup>6</sup>, C. L. Naumann<sup>18</sup>, M. de Naurois<sup>15</sup>, J. Niemiec<sup>34</sup>, S. J. Nolan<sup>8</sup>, L. Oakes<sup>6</sup>, S. Ohm<sup>33</sup>, E. de Oña Wilhelmi<sup>2</sup>, B. Opitz<sup>1</sup>, M. Ostrowski<sup>37</sup>, I. Oya<sup>6</sup>, M. Panter<sup>2</sup>, R. D. Parsons<sup>2</sup>, M. Paz Arribas<sup>6</sup>, N. W. Pekeur<sup>16</sup>, G. Pelletier<sup>32</sup>, J. Perez<sup>14</sup>, P.-O. Petrucci<sup>32</sup>, B. Peyaud<sup>20</sup>, S. Pita<sup>31</sup>, H. Poon<sup>2</sup>, G. Pühlhofer<sup>19</sup>, M. Punch<sup>31</sup>, A. Quirrenbach<sup>24</sup>, S. Raab<sup>7</sup>, M. Raue<sup>1</sup>, A. Reimer<sup>14</sup>, O. Reimer<sup>14</sup>, M. Renaud<sup>35</sup>, R. de los Reyes<sup>2</sup>, F. Rieger<sup>2</sup>, L. Rob<sup>40</sup>, C. Romoli<sup>3</sup>, S. Rosier-Lees<sup>36</sup>, G. Rowell<sup>30</sup>, B. Rudak<sup>11</sup>, C. B. Rulten<sup>17</sup>, V. Sahakian<sup>5,4</sup>, D. A. Sanchez<sup>2,36</sup>, A. Santangelo<sup>19</sup>, R. Schlickeiser<sup>13</sup>, F. Schüssler<sup>20</sup>, A. Schulz<sup>9</sup>, U. Schwanke<sup>6</sup>, S. Schwarzburg<sup>19</sup>, S. Schwemmer<sup>24</sup>, H. Sol<sup>17</sup>, G. Spengler<sup>6</sup>, F. Spies<sup>1</sup>, Ł. Stawarz<sup>37</sup>, R. Steenkamp<sup>29</sup>, C. Stegmann<sup>10,9</sup>, F. Stinzinger<sup>7</sup>, K. Stycz<sup>9,\*</sup>, I. Sushch<sup>6,16</sup>, A. Szostek<sup>37</sup>, J.-P. Tavernet<sup>18</sup>, T. Tavernier<sup>31</sup>, A. M. Taylor<sup>3</sup>, R. Terrier<sup>31</sup>, M. Tluczykont<sup>1</sup>, C. Trichard<sup>36</sup>, K. Valerius<sup>7</sup>, C. van Eldik<sup>7</sup>, B. van Soelen<sup>39</sup>, G. Vasileiadis<sup>35</sup>, C. Venter<sup>16</sup>, A. Viana<sup>2</sup>, P. Vincent<sup>18</sup>, H. J. Völk<sup>2</sup>, F. Volpe<sup>2</sup>, M. Vorster<sup>16</sup>, T. Vuillaume<sup>32</sup>, S. J. Wagner<sup>24</sup>, P. Wagner<sup>6</sup>, M. Ward<sup>8</sup>, M. Weidinger<sup>13</sup>, Q. Weitzel<sup>2</sup>, R. White<sup>33</sup>, A. Wierzcholska<sup>37</sup>, P. Willmann<sup>7</sup>, A. Wörnlein<sup>7</sup>, D. Wouters<sup>20</sup>, V. Zabalza<sup>2</sup>, M. Zacharias<sup>13</sup>, A. Zajczyk<sup>11,35</sup>, A. A. Zdziarski<sup>11</sup>, A. Zech<sup>17</sup>, and H.-S. Zechlin<sup>1</sup>

(Affiliations can be found after the references)

Received 8 November 2013 / Accepted 18 January 2014

### ABSTRACT

**Context.** On March 4, 2013 the *Fermi*-LAT and AGILE reported a flare from the direction of the Crab nebula in which the high-energy (HE;  $E > 100$  MeV) flux was six times above its quiescent level. Simultaneous observations in other energy bands give us hints about the emission processes during the flare episode and the physics of pulsar wind nebulae in general.

**Aims.** We search for variability in the emission of the Crab nebula at very-high energies (VHE;  $E > 100$  GeV), using contemporaneous data taken with the H.E.S.S. array of Cherenkov telescopes.

**Methods.** Observational data taken with the H.E.S.S. instrument on five consecutive days during the flare were analysed for the flux and spectral shape of the emission from the Crab nebula. Night-wise light curves are presented with energy thresholds of 1 TeV and 5 TeV.

**Results.** The observations conducted with H.E.S.S. on March 6 to March 10, 2013 show no significant changes in the flux. They limit the variation in the integral flux above 1 TeV to less than 63% and the integral flux above 5 TeV to less than 78% at a 95% confidence level.

**Key words.** gamma rays: ISM – ISM: individual objects: Crab nebula – radiation mechanisms: non-thermal – relativistic processes

\* Corresponding authors: [arnim.balzer;dieter.horns;kornelia.stycz]@desy.de

## 1. Introduction

The Crab nebula (for an overview see [Hester 2008](#)) is a pulsar wind nebula (PWN) powered by the Crab pulsar (in the following, the name *Crab* is used synonymously for the system of the Crab pulsar and its nebula). The rotational energy of the pulsar is converted into kinetic energy of a relativistic pair-plasma flow terminating in a shock with subsequent particle acceleration ([Rees & Gunn 1974](#)). Unpulsed emission from the downstream flow (the nebula) covers all observable wavelengths. The electrons and positrons of the plasma emit synchrotron radiation from radio wavelengths up to several hundred MeV, and they Compton-upscatter ambient photons (see e.g. [de Jager & Harding 1992](#); and [Atoyan & Aharonian 1996](#)) up to energies of at least 80 TeV ([Aharonian et al. 2004](#)).

These processes manifest themselves as clearly distinguishable peaks in the spectral energy distribution, which intersect in the energy band observed with *Fermi*-LAT ([Abdo et al. 2010](#)), AGILE ([Tavani et al. 2009](#)) and EGRET ([Kuiper et al. 2001](#)). Although the Crab is treated as a standard candle in very-high-energy (VHE;  $E > 100$  GeV)  $\gamma$ -ray astronomy (e.g. [Meyer et al. 2010](#)), its emission shows substantial variability at high energies (HE;  $E > 100$  MeV) (see e.g. [Tavani et al. 2011](#); [Abdo et al. 2011](#); [Striani et al. 2011, 2013b](#); [Buehler et al. 2012](#)), as well as at X-ray energies ([Wilson-Hodge et al. 2011](#)), albeit with a smaller relative amplitude of flux changes ( $\approx 5\%$ ) and on longer time scales of a few months. The most recent example is the flare detected with *Fermi*-LAT ([Ojha et al. 2013](#); [Meyer et al. 2013](#)) and AGILE ([Striani et al. 2013a](#); [Verrecchia et al. 2013](#)) in March 2013, when the peak photon flux of the synchrotron component above 100 MeV was  $(103.4 \pm 0.8) \times 10^{-7} \text{ cm}^{-2} \text{ s}^{-1}$  compared to  $(6.1 \pm 0.1) \times 10^{-7} \text{ cm}^{-2} \text{ s}^{-1}$  in its quiescent state, and variability was measured on time scales of a few hours.

As in previous flares (see e.g. [Buehler et al. 2012](#)), the higher flux state in March 2013 was accompanied by a hardening of the spectrum in the HE part of the synchrotron energy range. Generally, this implies either enhanced production of electrons and positrons or changes in the magnetic and electric fields. While in the latter case, the inverse-Compton (IC) component will largely remain unchanged, in the former, the flare observed at a synchrotron energy  $E_{\text{syn}}$  is accompanied by a flare at a corresponding energy  $E_{\text{IC}}$  of IC scattered ambient photons. The apparent observed energy  $E_{\text{syn}}$  of a few hundred MeV exceeds the maximum achievable energy of synchrotron radiation from shock-accelerated electrons/positrons ([Guilbert et al. 1983](#); [de Jager et al. 1996](#); [Lyutikov 2010](#)). This observation indicates the presence of a mild Doppler boost or a different acceleration mechanism altogether ([Lyutikov 2010](#); [Cerutti et al. 2013](#)). Observations at the VHE band during flaring episodes provide additional information on the conditions in the emission region (e.g. magnetic field, Doppler boost). In specific model scenarios, the relative variability expected at TeV energies accompanying a major outburst at GeV energies ranges from  $10^{-2}$  (see e.g. Fig. 8 in [Lobanov et al. 2011](#)) to unity and higher (see e.g. [Bednarek & Idec 2011](#); [Kohri et al. 2012](#)). The detection of variability in the Crab nebula with H.E.S.S. is mainly limited by systematic uncertainties on the flux measurement of  $\sim 20$ – $30\%$ . In addition, statistics rapidly decrease with increasing energy.

Given that the origin of the flares is poorly understood, the search for VHE counterparts of the flares is of great interest. Moreover, the ARGO-YBJ group claimed nearly four times higher event rates than average over a period of eight days ([Aielli et al. 2010](#)) during a flare observed with AGILE ([Tavani et al. 2010](#)) and *Fermi*-LAT ([Buehler et al. 2010](#)) in September 2010.

Whether the reported signals have an astrophysical origin that belongs to the Crab nebula remains unsettled, pending independent confirmation with other instruments. The contemporaneous observations of the Crab nebula in March 2013 provide the opportunity to study the emission during a flaring state at multiple wavelengths, ranging from infrared to X-rays ([Mayer et al. 2013](#)) and VHE ([Aliu et al. 2014](#) and H.E.S.S. observations reported in this paper). Spectral measurements at multi-TeV energies, which are most relevant in the search for an IC component, are required to complement our understanding of the flaring Crab nebula and facilitate broadband modelling. The highest sensitivity for multi-TeV  $\gamma$  rays is reached with ground-based Cherenkov telescope observations at high zenith angles, since the inclination angle of the induced air showers results in large effective areas. Since the Crab nebula culminates at  $45^\circ$  for H.E.S.S., it provides the best observation conditions of all ground-based  $\gamma$ -ray telescopes.

## 2. Data set and analysis

The High Energy Stereoscopic System (H.E.S.S.) is an array of five Imaging Air Cherenkov telescopes situated in the Khomas Highland, Namibia, at 1800 m above sea level. Since 2004, four telescopes (H.E.S.S. Phase I) with mirror surfaces of  $\sim 100 \text{ m}^2$  each have been detecting air showers produced by  $\gamma$  rays with energies higher than 100 GeV ([Hinton 2004](#)). This array forms a square of 120 m side length. It has a field of view of  $5^\circ$  in diameter and a relative energy resolution of  $\sim 14\%$  at 1 TeV ([Aharonian et al. 2006](#)). In September 2012, a fifth telescope placed in the middle of the original square was inaugurated, initiating H.E.S.S. Phase II. It has a mirror surface of  $\sim 600 \text{ m}^2$  and lowers the energy threshold of H.E.S.S. to tens of GeV.

Due to the flare, *Fermi*-LAT was switched to pointed target-of-opportunity observation mode of the Crab between MJD 56 355 and 56 359 ([Meyer et al. 2013](#)). The data presented here are ten observation runs taken in or shortly after this period, when the flux measured by *Fermi*-LAT was still about twice its average value. The data are comprised of runs with either three or four of the H.E.S.S. I telescopes, each lasting 28 min. Since it was the rainy season in Namibia, observations were possible only during a few nights. In this period of time, the Crab nebula was visible at large zenith angles for H.E.S.S. (see Table 1).

The data were analysed with the H.E.S.S. Analysis Package<sup>1</sup> for shower reconstruction and a multivariate analysis ([Ohm et al. 2009](#)) applying  $\zeta$  *std-cuts* for suppression of the hadronic background. To estimate the cosmic-ray background, the *reflected region* method ([Berge et al. 2007](#)) was used. Significances (in standard deviations,  $\sigma$ ) were calculated using Eq. (17) in [Li & Ma \(1983\)](#). The analysis results for each night and for the whole data set can be found in Table 1. A cross-check with an independent analysis ([de Naurois & Rolland 2009](#)) and an independent data calibration indicates that the systematic error on the flux normalisation is 30% for this data set, which is taken into account in the calculation of flux upper limits shown below.

## 3. Results

Analysing the complete sample of ten runs taken in the nights from March 6 to March 10, 2013 (MJD 56358–MJD 56365), we obtained an acceptance-corrected live time of 4.4 h, yielding 754 excess events from the source region. A simple power law and an exponential cut-off power law were considered to

<sup>1</sup> HAP version hap-12-03-pl02.

**Table 1.** Analysis results and for each night and the complete data set.

Date	MJD	$T_{\text{live}}$ (s)	$Z_{\text{mean}}$ (deg.)	$N_{\text{ON}}$	$N_{\text{OFF}}$	Excess	Sign. $\sigma$	$I_0$ (1 TeV)	Index	Flux >1 TeV	Flux >5 TeV
2013	-56 300										
03-06	57.8	3181	54	202	498	175	20	$3.5 \pm 0.5$	$2.6 \pm 0.1$	$1.89 \pm 0.19$	$0.11 \pm 0.03$
03-07	58.8	3152	52	223	455	198	23	$4.2 \pm 0.4$	$2.8 \pm 0.1$	$2.37 \pm 0.21$	$0.08 \pm 0.03$
03-08	59.8	3155	53	184	460	159	19	$3.5 \pm 0.5$	$2.6 \pm 0.1$	$2.24 \pm 0.21$	$0.18 \pm 0.04$
03-09	60.8	4827	55	199	557	169	19	$3.3 \pm 0.5$	$2.7 \pm 0.1$	$1.76 \pm 0.18$	$0.12 \pm 0.03$
03-13	64.8	1596	54	62	173	53	11	$5.2 \pm 1.4$	$3.4 \pm 0.3$	$2.06 \pm 0.36$	$0.06 \pm 0.05$
Full set	-	15911	54	870	2143	754	42	$3.8 \pm 0.2$	$2.7 \pm 0.1$	$2.14 \pm 0.10$	$0.12 \pm 0.01$

**Notes.** Modified Julian date (MJD) of the start of the observation, live-time ( $T_{\text{live}}$ ), mean zenith angle ( $Z_{\text{mean}}$ ), the number of ON and OFF source events, the excess and its significance. The normalisation at 1 TeV ( $I_0$ ) is given in units of ( $10^{-11} \text{ cm}^{-2} \text{ s}^{-1} \text{ TeV}^{-1}$ ) and integral fluxes above 1 TeV and above 5 TeV in units of  $10^{-11} \text{ cm}^{-2} \text{ s}^{-1}$ . The underlying spectral model was assumed to be a power law. The given errors are statistical ones. The estimated systematic errors are 30% for all fluxes and 0.1 for spectral indices.

model the energy distribution, motivated by previous publications (Aharonian et al. 2006). Low statistics for  $E > 10$  TeV, however, made it impossible to distinguish between an exponential cut-off and a simple power law model. This is not a characteristic of this specific data set: A sample of ten runs on the Crab nebula from another period with similar telescope participation did not allow any discrimination between a power law model and a power law model with an exponential cut-off, either. Therefore, the numerically more stable power law model was adopted for all spectra and fitted in the energy range [0.681–46.46] TeV. The energy spectrum of the complete sample is shown in Fig. 2, together with the exponential cut-off power law spectrum taken from Aharonian et al. (2006) as a reference. Night-wise data were fitted with a power law model as well, and all results and their statistical errors are compiled in Table 1. The spectral analysis results of both night-wise and complete samples agree with Aharonian et al. (2006), where an exponential cut-off power law was the best-fitting spectral model with  $I_0(1 \text{ TeV}) = (3.76 \pm 0.07) \times 10^{-11} \text{ cm}^{-2} \text{ s}^{-1} \text{ TeV}^{-1}$ ,  $\Gamma_\gamma = 2.39 \pm 0.03$ , and  $E_{\text{cutoff}} = (14.3 \pm 2.1) \text{ TeV}$ .

To test for the compatibility of this spectrum with the spectrum of the flare data set presented here, a  $\chi^2$ -test was conducted. Under the optimistic assumption of cancelling systematics between both data sets, the spectrum from Aharonian et al. (2006) served as the null hypothesis for testing the photon spectrum above 1 TeV, 5 TeV, and 10 TeV, resulting in  $\chi^2/\text{ndf}$  values of 32.6/31, 15.7/14, and 5.0/7, respectively. These values indicate no significant difference in the spectra. Due to the low statistics in the last bin of the spectrum (four ON events, one OFF event) a likelihood profile was calculated as described in Rolke et al. (2005). With this method, a deviation of the last spectrum point from the expected flux according to Aharonian et al. (2006) is about  $2.5\sigma$ , including neither systematic uncertainties nor the statistic uncertainties on the spectrum from Aharonian et al. (2006).

Since a flare in the MeV energy band is expected to be accompanied by an enhanced flux at tens of TeV (Lobanov et al. 2011), a search for variations in the flux above different energy thresholds was conducted. Integral fluxes above 1 TeV and 5 TeV were calculated for the night-wise samples (see Fig. 1), and higher energy thresholds were tested but are non-restrictive owing to low statistics. Fits of constants to the night-wise flux measurements give values of  $(2.0 \pm 0.1) \times 10^{-11} \text{ cm}^{-2} \text{ s}^{-1}$  with  $\chi^2/\text{ndf} = 6.1/4$  and  $(0.11 \pm 0.1) \times 10^{-11} \text{ cm}^{-2} \text{ s}^{-1}$  with  $\chi^2/\text{ndf} = 1.2/4$  for an energy threshold of 1 TeV and 5 TeV, respectively. For comparison, the integral fluxes of the spectrum published in Aharonian et al. (2006) above 1 TeV and above 5 TeV are

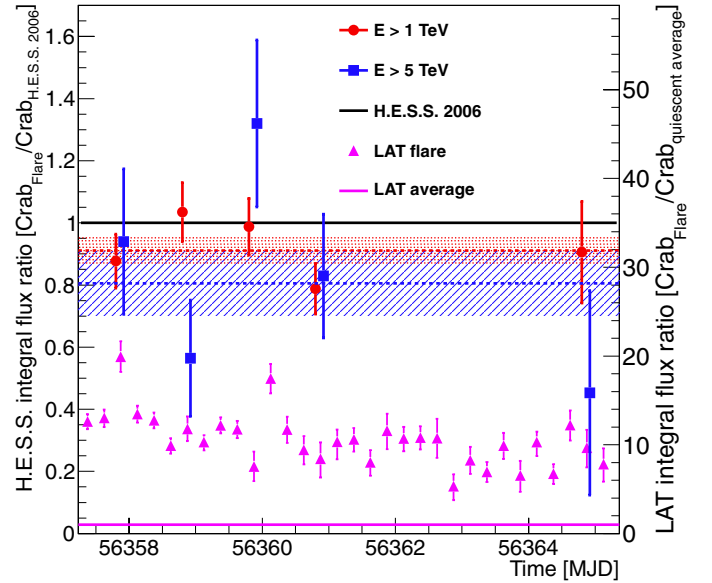


**Fig. 1.** Night-wise light curves for energy thresholds of 1 and 5 TeV. Red squares indicate integral fluxes >1 TeV relative to the integral flux above 1 TeV obtained from Aharonian et al. (2006). Error bars depict  $1\sigma$  statistical errors. The dashed red line is the fit of a constant to this light curve, and the hatched red area marks the  $1\sigma$  statistical error. The equivalent data for an energy threshold of 5 TeV are presented in blue. For reference, the *Fermi*-LAT synchrotron light curve as published in Mayer et al. (2013) is shown in magenta. Each bin corresponds to 6 h of observations. The flux is scaled to the average quiescent synchrotron photon flux as reported in Buehler et al. (2012) ( $(6.1 \pm 0.2) \times 10^{-7} \text{ cm}^{-2} \text{ s}^{-1}$ ).

$(2.26 \pm 0.08) \times 10^{-11} \text{ cm}^{-2} \text{ s}^{-1}$  and  $(0.14 \pm 0.01) \times 10^{-11} \text{ cm}^{-2} \text{ s}^{-1}$ , respectively.

The first night of H.E.S.S. observations (MJD 56 358) is coincident with the highest flux level detected by *Fermi*-LAT in the March 2013 period of enhanced flux (Mayer et al. 2013). For that reason, upper limits on an enhancement of integral fluxes above 1 TeV and above 5 TeV were calculated for that night by comparison with the integral flux of the spectrum published in Aharonian et al. (2006). The spectrum in Aharonian et al. (2006) was produced with a different analysis and under different observation conditions; therefore, event-number based upper limit calculations as put forward in Rolke et al. (2005) cannot be applied. Instead, the two flux values  $F_{2006}$  and  $F_{2013}$ , determined by integration of the fitted spectral functions, are compared, which automatically takes energy migrations and efficiencies correctly

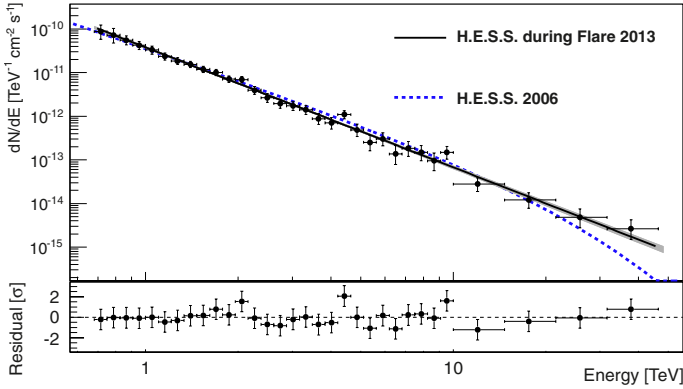


**Fig. 2.** Crab photon spectrum. Black circles indicate the H.E.S.S. Crab nebula data taken in the nights from March 6 to March 10, 2013 with  $1\sigma$  error bars on the flux in the respective bin. The black line and the grey shaded area are the fitted power law model and the corresponding  $1\sigma$  error butterfly. The blue dashed line corresponds to the spectrum reported in Aharonian et al. (2006).

into account. Since no significant deviation of  $F_{2006}$  and  $F_{2013}$  is found, and  $F_{2006} > F_{2013}$ , a conservative 95% confidence level upper limit is determined as  $F_{2006} + 2\sigma$ , where  $\sigma$  comprises the quadratically added statistical and systematic errors. With this method, the upper limit on an enhancement of the integrated flux above 1 TeV for the first night is  $3.66 \times 10^{-11} \text{ cm}^{-2} \text{ s}^{-1}$  at a 95% confidence level, corresponding to an enhancement factor of 1.63 compared to the integrated flux published in Aharonian et al. (2006). For the integrated flux above 5 TeV, the upper limit on the flux enhancement factor relative to the integrated flux above 5 TeV as published in Aharonian et al. (2006) is 1.78 at a 95% confidence level.

#### 4. Conclusions

The upper limits on the enhancement of the Crab flux are far above what is expected for the TeV energy range from some models, which predict enhancement factors of at most 1.01, as described above referring to Lobanov et al. (2011). In scenarios as in Bednarek & Idec (2011) or Kohri et al. (2012), however, enhancement factors of 2 or more are possible, exceeding the upper limits presented here. Besides this, experimental evidence does exist for such a high relative flux variability: During the flare discovered by AGILE in September 2010 (Tavani et al. 2010), three to four times the average Crab flux at a mean energy of 1 TeV was reported by ARGO-YBJ for ten days with an observation time of about 5.5 h each (Aielli et al. 2010). On July 3, 2012 ARGO-YBJ even observed an enhancement of eight times the average flux (Bartoli et al. 2012) for a flare reported by *Fermi* on that day (Ojha et al. 2012). Such an increase in flux clearly lies above the upper limits presented in this paper and could be observed by the H.E.S.S. instrument if it was present during the observations at hand, rendering it unlikely. More recently, the ARGO-YBJ group claimed a correlation of their Crab flux measurements with the varying *Fermi*-LAT flux and an average flux enhancement factor of  $2.4 \pm 0.8$  during flares at GeV energies (Vernetto 2013). This value is compatible with the  $2\sigma$  upper limits presented here only at the lower bound of its  $1\sigma$  errors.

On the other hand, both the MAGIC and VERITAS imaging atmospheric Cherenkov telescopes did not detect any flaring activity at VHE either during previous flares or during the period investigated in this paper. These instruments use observation times in units of  $\sim 30$  min, very similar to H.E.S.S. For the flare in September 2010, both MAGIC and VERITAS did not detect

any flux enhancement in 58 min during one night and 120 min during four nights, respectively (Mariotti 2010; Ong 2010). For the flaring period discussed here, an integral flux above 1 TeV of  $(2.05 \pm 0.07) \times 10^{-11} \text{ cm}^{-2} \text{ s}^{-1}$  was reported by VERITAS for a period of ten days with 10.3 h of observations in total, compared to an integral flux of  $(2.10 \pm 0.06) \times 10^{-11} \text{ cm}^{-2} \text{ s}^{-1}$  for observations outside the flare time window (Aliu et al. 2014). Taking the 30% systematic error on flux measurements with VERITAS into account (Aliu et al. 2014), these numbers are in perfect agreement with the upper limits presented here and they give a very similar constraint on a possible flux enhancement.

The *Fermi*-LAT energy spectra of the flaring component extending to energies of a few hundred MeV favour at least a modest Doppler boosting. High angular resolution observations of moving features in the nebula, however, do not show direct evidence for bulk flow with  $v > 0.5c$ . It has been suggested that modest Doppler factors could be realised at the region close to the termination shock and that the optically resolved knot  $0.6''$  displaced from the pulsar could be responsible for the  $\gamma$ -ray variability (Komissarov & Lyutikov 2011). In this scenario, the Doppler boost would lead to an apparent enhancement of the inverse-Compton component for the stationary observer. Not observing a transient feature at optical or X-ray frequencies Weisskopf et al. (2013) during the flare is consistent with this picture given that the extrapolation of the observed  $\gamma$ -ray spectrum to lower energies would render the X-ray/optical counterpart invisible against the bright nebula emission. Furthermore, a rather high value of the minimum energy of the radiating electrons would basically lead to no sizeable emission at lower energies.

Assuming that the specific flux of the flare follows a power law  $f_\nu \propto \nu^{-\alpha}$ , the ratio of inverse-Compton and synchrotron emission at fixed frequencies scales with  $f_\nu^{\text{IC}}/f_\nu^{\text{Syn}} \propto (\delta/B)^{1+\alpha}$  (Dermer et al. 1997; Georganopoulos et al. 2002), with  $\delta$  the relativistic Doppler factor and  $B$  the average magnetic field in the emission region. Therefore, the H.E.S.S. constraint combined with the contemporaneously measured *Fermi*-LAT (synchrotron) flux limits  $\delta \lesssim 100(B/122 \mu\text{G})$ .

Future multi-wavelength measurements, especially with instruments with larger collection areas for TeV  $\gamma$  rays like the planned Cherenkov telescope array, will be able to constrain such models even further.

*Acknowledgements.* The support of the Namibian authorities and of the University of Namibia in facilitating the construction and operation of H.E.S.S. is gratefully acknowledged, as is the support by the German Ministry for Education and Research (BMBF), the Max Planck Society, the German Research Foundation (DFG), the French Ministry for Research, the CNRS-IN2P3 and the Astroparticle Interdisciplinary Programme of the CNRS, the UK Science and Technology Facilities Council (STFC), the IPNP of the Charles University, the Czech Science Foundation, the Polish Ministry of Science and Higher Education, the South African Department of Science and Technology and National Research Foundation, and by the University of Namibia. We appreciate the excellent work of the technical support staff in Berlin, Durham, Hamburg, Heidelberg, Palaiseau, Paris, Saclay, and in Namibia in the construction and operation of the equipment.

#### References

- Abdo, A. A., Ackermann, M., Ajello, M., et al. 2010, *ApJ*, 708, 1254
- Abdo, A. A., Ackermann, M., Ajello, M., et al. 2011, *Science*, 331, 739
- Aharonian, F., Akhperjanian, A. G., Bazer-Bachi, A. R., et al. 2006, *A&A*, 457, 899
- Aielli, G., Camarri, P., Iuppa, R., et al. 2010, *ATel*, 2921, 1
- Aharonian, F., Akhperjanian, A. G., & the HEGRA Collaboration. 2004, *ApJ*, 614, 897
- Aliu, E., Archambault, S., et al. (the VERITAS Collaboration) 2014, *ApJ*, 781, L11
- Atayan, A. M., & Aharonian, F. A. 1996, *MNRAS*, 278, 525

- Bartoli, B., Bernardini, P., Bi, X. J., et al. 2012, *ATel*, 4258, 1
- Bednarek, W., & Idec, W. 2011, *MNRAS*, 414, 2229
- Berge, D., Funk, S., & Hinton, J. 2007, *A&A*, 466, 1219
- Buehler, R., D'Ammando, F., & Hays, E. 2010, *ATel*, 2861, 1
- Buehler, R., Scargle, J. D., Blandford, R. D., et al. 2012, *ApJ*, 749, 26
- Cerutti, B., Werner, G. R., Uzdensky, D. A., & Begelman, M. C. 2013, *ApJ*, 770, 147
- de Jager, O. C., & Harding, A. K. 1992, *ApJ*, 396, 161
- de Jager, O. C., Harding, A. K., Michelson, P. F., et al. 1996, *ApJ*, 457, 253
- de Naurois, M., & Rolland, L. 2009, *Astropart. Phys.*, 32, 231
- Dermer, C. D., Sturmer, S. J., & Schlickeiser, R. 1997, *ApJS*, 109, 103
- Georgantopoulos, M., Aharonian, F. A., & Kirk, J. G. 2002, *A&A*, 388, L25
- Guilbert, P. W., Fabian, A. C., & Rees, M. J. 1983, *MNRAS*, 205, 593
- Hester, J. J. 2008, *ARA&A*, 46, 127
- Hinton, J. A. 2004, *New Astron. Rev.*, 48, 331
- Kohri, K., Ohira, Y., & Ioka, K. 2012, *MNRAS*, 424, 2249
- Komissarov, S. S., & Lyutikov, M. 2011, *MNRAS*, 414, 2017
- Kuiper, L., Hermsen, W., Cusumano, G., et al. 2001, *A&A*, 378, 918
- Li, T., & Ma, Y. 1983, *ApJ*, 272, 317
- Lobanov, A. P., Horns, D., & Muxlow, T. W. B. 2011, *A&A*, 533, A10
- Lyutikov, M. 2010, *MNRAS*, 405, 1809
- Mariotti, M. 2010, *ATel*, 2967, 1
- Mayer, M., Buehler, R., Hays, E., et al. 2013, *ApJ*, 775, L37
- Meyer, M., Horns, D., & Zechlin, H.-S. 2010, *A&A*, 523, A2
- Ohm, S., van Eldik, C., & Egberts, K. 2009, *Astropart. Phys.*, 31, 383
- Ojha, R., Buehler, R., Hays, E., & Dutka, M. 2012, *ATel*, 4239, 1
- Ojha, R., Hays, E., Buehler, R., & Dutka, M. 2013, *ATel*, 4855, 1
- Ong, R. A. 2010, *ATel*, 2968, 1
- Rees, M. J., & Gunn, J. E. 1974, *MNRAS*, 167, 1
- Rolke, W. A., López, A. M., & Conrad, J. 2005, *Nucl. Instr. Meth. Phys. Res. A*, 551, 493
- Striani, E., Tavani, M., Piano, G., et al. 2011, *ApJ*, 741, L5
- Striani, E., Tavani, M., Verrecchia, F., et al. 2013a, *ATel*, 4856, 1
- Striani, E., Tavani, M., Vittorini, V., et al. 2013b, *ApJ*, 765, 52
- Tavani, M., Barbiellini, G., Argan, A., et al. 2009, *A&A*, 502, 995
- Tavani, M., Striani, E., Bulgarelli, A., et al. 2010, *ATel*, 2855, 1
- Tavani, M., Bulgarelli, A., Vittorini, V., et al. 2011, *Science*, 331, 736
- Vernetto, S. F. 2013 [[arXiv:1307.7041](https://arxiv.org/abs/1307.7041)]
- Verrecchia, F., Striani, E., Tavani, M., et al. 2013, *ATel*, 4867, 1
- Weisskopf, M. C., Tennant, A. F., Arons, J., et al. 2013, *ApJ*, 765, 56
- Wilson-Hodge, C. A., Cherry, M. L., Case, G. L., et al. 2011, *ApJ*, 727, L40
- <sup>1</sup> Universität Hamburg, Institut für Experimentalphysik, Luruper Chaussee 149, 22761 Hamburg, Germany
- <sup>2</sup> Max-Planck-Institut für Kernphysik, PO Box 103980, 69029 Heidelberg, Germany
- <sup>3</sup> Dublin Institute for Advanced Studies, 31 Fitzwilliam Place, 2 Dublin, Ireland
- <sup>4</sup> National Academy of Sciences of the Republic of Armenia, Yerevan
- <sup>5</sup> Yerevan Physics Institute, 2 Alikhanian Brothers St., 375036 Yerevan, Armenia
- <sup>6</sup> Institut für Physik, Humboldt-Universität zu Berlin, Newtonstr. 15, 12489 Berlin, Germany
- <sup>7</sup> Universität Erlangen-Nürnberg, Physikalisches Institut, Erwin-Rommel-Str. 1, 91058 Erlangen, Germany
- <sup>8</sup> University of Durham, Department of Physics, South Road, Durham DH1 3LE, UK
- <sup>9</sup> DESY, 15738 Zeuthen, Germany
- <sup>10</sup> Institut für Physik und Astronomie, Universität Potsdam, Karl-Liebknecht-Strasse 24/25, 14476 Potsdam, Germany
- <sup>11</sup> Nicolaus Copernicus Astronomical Center, ul. Bartycka 18, 00-716 Warsaw, Poland
- <sup>12</sup> Department of Physics and Electrical Engineering, Linnaeus University, 351 95 Växjö, Sweden
- <sup>13</sup> Institut für Theoretische Physik, Lehrstuhl IV: Weltraum und Astrophysik, Ruhr-Universität Bochum, 44780 Bochum, Germany
- <sup>14</sup> Institut für Astro- und Teilchenphysik, Leopold-Franzens-Universität Innsbruck, 6020 Innsbruck, Austria
- <sup>15</sup> Laboratoire Leprince-Ringuet, École Polytechnique, CNRS/IN2P3, 91128 Palaiseau, France
- <sup>16</sup> Centre for Space Research, North-West University, 2520 Potchefstroom, South Africa
- <sup>17</sup> LUTH, Observatoire de Paris, CNRS, Université Paris Diderot, 5 place Jules Janssen, 92190 Meudon, France
- <sup>18</sup> LPNHE, Université Pierre et Marie Curie Paris 6, Université Denis Diderot Paris 7, CNRS/IN2P3, 4 place Jussieu, 75252, Paris Cedex 5, France
- <sup>19</sup> Institut für Astronomie und Astrophysik, Universität Tübingen, Sand 1, 72076 Tübingen, Germany
- <sup>20</sup> DSM/Irfu, CEA Saclay, 91191 Gif-Sur-Yvette Cedex, France
- <sup>21</sup> Astronomical Observatory, The University of Warsaw, Al. Ujazdowskie 4, 00-478 Warsaw, Poland
- <sup>22</sup> now at Harvard-Smithsonian Center for Astrophysics, 60 garden Street, Cambridge MA, 02138, USA
- <sup>23</sup> School of Physics, University of the Witwatersrand, 1 Jan Smuts Avenue, Braamfontein, 2050 Johannesburg, South Africa
- <sup>24</sup> Landessternwarte, Universität Heidelberg, Königstuhl, 69117 Heidelberg, Germany
- <sup>25</sup> Oskar Klein Centre, Department of Physics, Stockholm University, Albanova University Center, 10691 Stockholm, Sweden
- <sup>26</sup> Wallenberg Academy Fellow
- <sup>27</sup> Université Bordeaux 1, CNRS/IN2P3, Centre d'Études Nucléaires de Bordeaux Gradignan, 33175 Gradignan, France
- <sup>28</sup> Funded by contract ERC-StG-259391 from the European Community
- <sup>29</sup> University of Namibia, Department of Physics, Private Bag 13301, Windhoek, Namibia
- <sup>30</sup> School of Chemistry & Physics, University of Adelaide, Adelaide 5005, Australia
- <sup>31</sup> APC, AstroParticule et Cosmologie, Université Paris Diderot, CNRS/IN2P3, CEA/Irfu, Observatoire de Paris, Sorbonne Paris Cité, 10 rue Alice Domon et Léonie Duquet, 75205 Paris Cedex 13, France
- <sup>32</sup> UJF-Grenoble 1/CNRS-INSU, Institut de Planétologie et d'Astrophysique de Grenoble (IPAG) UMR 5274, 38041 Grenoble, France
- <sup>33</sup> Department of Physics and Astronomy, The University of Leicester, University Road, Leicester, LE1 7RH, UK
- <sup>34</sup> Instytut Fizyki Jądrowej PAN, ul. Radzikowskiego 152, 31-342 Kraków, Poland
- <sup>35</sup> Laboratoire Univers et Particules de Montpellier, Université Montpellier 2, CNRS/IN2P3, CC 72, Place Eugène Bataillon, 34095 Montpellier Cedex 5, France
- <sup>36</sup> Laboratoire d'Annecy-le-Vieux de Physique des Particules, Université de Savoie, CNRS/IN2P3, 74941 Annecy-le-Vieux, France
- <sup>37</sup> Obserwatorium Astronomiczne, Uniwersytet Jagielloński, ul. Orła 171, 30-244 Kraków, Poland
- <sup>38</sup> Toruń Centre for Astronomy, Nicolaus Copernicus University, ul. Gagarina 11, 87-100 Toruń, Poland
- <sup>39</sup> Department of Physics, University of the Free State, PO Box 339, 9300 Bloemfontein, South Africa
- <sup>40</sup> Charles University, Faculty of Mathematics and Physics, Institute of Particle and Nuclear Physics, V Holešovičkách 2, 180 00 Prague 8, Czech Republic